

Correcting MODIS aerosol optical depth products using a ridge regression model

Renlong Hang, Qingshan Liu, Guiyu Xia & Huihui Song

To cite this article: Renlong Hang, Qingshan Liu, Guiyu Xia & Huihui Song (2018) Correcting MODIS aerosol optical depth products using a ridge regression model, International Journal of Remote Sensing, 39:10, 3275-3286, DOI: [10.1080/01431161.2018.1439597](https://doi.org/10.1080/01431161.2018.1439597)

To link to this article: <https://doi.org/10.1080/01431161.2018.1439597>



Published online: 15 Feb 2018.



Submit your article to this journal [↗](#)



View related articles [↗](#)



View Crossmark data [↗](#)



Correcting MODIS aerosol optical depth products using a ridge regression model

Renlong Hang, Qingshan Liu, Guiyu Xia and Huihui Song

Jiangsu Key Laboratory of Big Data Analysis Technology, School of Information and Control, Nanjing University of Information Science and Technology, Nanjing, China

ABSTRACT

Aerosol optical depth (AOD) is an important metric for the concentration of aerosols in the atmosphere. Dark target (DT) algorithm is a widely used physical model to retrieve AOD over land from Moderate Resolution Imaging Spectroradiometer (MODIS) data. However, due to the limitation of surface 'dark-target' in some regions and over certain surface types, it does not work very well. In this paper, we propose two hybrid frameworks based on ridge regression (RR) to improve the retrieval accuracy. They are serial and parallel approaches. In both frameworks, the DT algorithm is used as a baseline to derive an initial result, and the bias between the derived AOD and the ground-truth is corrected by the RR model. To validate the effectiveness of the proposed methods, we apply them on 3093 collocated MODIS and Aerosol Robotic Network (AERONET) observations, covering 10 stations at all available time in China. The obtained results demonstrate that the proposed methods can improve retrieval performance compared to the corresponding DT algorithm and the RR model.

ARTICLE HISTORY

Received 24 March 2017
Accepted 1 February 2018

1. Introduction

Aerosols are small solid or liquid particles suspended in the atmosphere. They can scatter and absorb solar radiance, and modify the microphysical and radiative properties of clouds. One of the biggest challenges of current climate research is to quantify the effect of aerosols on the Earth's radiation budget (Kaufman, Tanr, and Boucher 2002). As a primary aerosol optical parameter which represents the aerosol radiative extinction in the atmosphere, aerosol optical depth (AOD), therefore, is considered as a key factor to understand aerosol climate effects (Huang et al. 2015).

AOD data can be obtained from either ground-based instruments or satellite-based instruments. Ground-based measurements, such as Aerosol Robotic Network (AERONET) (Holben et al. 1998; Dubovik et al. 2000), can provide accurate aerosol information and enable frequent acquisition of data each day but only for individually discrete locations (Gao et al. 2016). Due to the high variation of aerosols in space and time, satellite observations, such as Moderate Resolution Imaging Spectroradiometer (MODIS) (King et al. 1992), are more suitable for deriving aerosol properties with greater spatial coverage.

In general, AERONET is often referred to as ground-truth to validate the satellite retrieval performance (Chu et al. 2002)

Since 2000, the MODIS instrument aboard the Terra satellite has been a major source of high-quality aerosol information. It observes reflected solar radiance through 36 spectral channels ranging from 414 nm to 14 μ m. The goal of retrieval is to derive AOD from the observed spectral values directly. Current operational MODIS retrieval model over land is the Collection 6 dark target (DT) algorithm (Levy et al. 2013). First, the measured top of the atmosphere (TOA) reflectance within each 10 km \times 10 km retrieval box is screened to remove unsuitable (e.g., cloudy, desert, snow/ice, inland water, and bright) pixels, and the DT pixels are identified in the 2.12 μ m channel. Second, an additional 20% darkest and 50% brightest pixels defined in the 0.66 μ m channel are discarded, and the remaining pixel-level reflectance is averaged. Finally, the TOA reflectance in the 2.12 μ m channel is related to surface reflectance at visible wavelengths (0.47 μ m and 0.66 μ m) via an assumed spectral/directional relationship, which are subsequently used to determine the total AOD from a weighted combination of fine-mode dominated and coarse-mode (dust) dominated aerosol models by matching the averaged TOA reflectance at these wavelengths.

However, due to the limitation of surface 'dark-target' in some regions and over certain surface types, DT algorithm does not work very well (Huang et al. 2015). Recently, some works about using machine learning models to retrieve AOD at given locations have been proposed (Vucetic et al. 2008; Lary et al. 2009; Hang et al. 2017; Gao et al. 2016). They aim to learn a mapping between AOD and satellite observations from data itself. These models often consist of two components. First is using the collocated satellite and ground-based observations to train a regression model. Then, the trained model is employed to predict AOD for satellite observations without ground-truth. Among various models, neural networks (NNs) (Vucetic et al. 2008; Ristovski, Vucetic, and Obradovic 2012) and support vector machines (SVMs) (Lary et al. 2009; Nguyen et al. 2011; Sun et al. 2016) are two popular ones, because they can accurately approximate complex non-linear relationships between satellite observations and ground-based observations. However, most of the existing machine learning models only take a part of the spectral values as features, resulting in the loss of effective information. Besides, the small number of available training data also degrades the performance of machine learning models. To address these issues, a graph regularized non-linear ridge regression model was proposed in (Hang et al. 2017), which obtains superior performances as compared to SVMs and NNs.

Machine learning models are data-driven methods without using any domain knowledge. They don't make any priori assumptions on variable relations or rigidly functional forms, and achieve higher performances than physical models (e.g., DT algorithm) if adequate amounts of training data are available. However, machine learning models encounter difficulties in retaining the physical explanations or structure knowledge of a physical system, because they are usually considered as black-box models, and their parameters do not generally represent physical parameters in a physical system. In contrast, physical models depend on the prior knowledge about the radiation transfer process. They have strong generalization capabilities and moderate retrieval performances. Recently, several works were proposed to fuse the prior knowledge of physical models into the machine learning models for simulating plant growth (Qu and Hu 2009;

Fan et al. 2015). Inspired by them, in this paper, we propose two hybrid frameworks to correct the MODIS AOD product. In both frameworks, the DT algorithm is used as a baseline to derive an initial result, and the bias between the derived AOD and the ground-truth is corrected by the RR model.

2. Data set

2.1. AERONET data

AERONET is a global network of about 850 ground-based instruments that observe aerosols (Holben et al. 1998). The instruments used are CIMEL spectral radiometers that measure direct-sun and diffuse-sky radiance, and determine AOD in different spectral bands centred on the nominal wavelengths of 340 nm, 440 nm, 670 nm, and others (Petrenko, Ichoku, and Leptoukh 2012). To facilitate inter-comparisons with other instruments, these data are interpolated to 550 nm using the quadratic fit on log-log scale from all wavelengths, at a particular location and time (Remer et al. 2005). We collect Level 2.0 cloud-screened AERONET AODs from ten stations at all available time in China. They are Beijing (39.98°N,116.38°E), XiangHe (39.75°N,116.96°E), Hangzhou-ZFU (30.26°N,119.73°E), Hefei (31.91°N,117.16°E), Hong_Kong_PolyU (22.30°N,114.18°E), Hong_Kong_Sheung (22.48°N,114.12°E), SACOL (35.95°N,104.14°E), Taihu (31.42°N,120.22°E), Xinglong (40.40°N,117.58°E), and Yulin (38.28°N,109.72°E) stations.

2.2. MODIS data

MODIS is a key instrument aboard the Terra satellite for the collection of aerosol and cloud information. It has a swath width of 2330 km, and achieves global coverage in about two days. The MODIS instrument has a single camera observing the TOA reflectance over 36 spectral channels at three different spatial resolutions (250 m, 500 m, 1 km). We obtain the MODIS Level-1B calibrated radiance product MOD021KM with a spatial resolution of 1 km, covering the same ten stations as AERONET data. Over the same spatial and temporal range, we obtain the Level-2 aerosol-retrieval product MOD04 with a spatial resolution of 10 km, a geolocation product MOD03 with 1 km resolution, and a cloud mask product MOD35 with a resolution of 1 km. Since the spatial resolution of MOD04 is different from that of MOD03 or MOD35, we need to magnify the MOD04 product by 10 times via a nearest-neighbor interpolation method.

2.3. Collocated AERONET-MODIS data

We obtain a total of 3093 spatially and temporally collocated observations from MODIS and AERONET at 10 stations. Consistent with the work in (Vucetic et al. 2008), each observation corresponds to a spatial region 30 km × 30 km surrounding an AERONET site, and the observation is generated if the following conditions are met: the region contains at least one non-cloud pixel, at least one MODIS AOD retrieval with quality assurance (QA) >1 is available, and at least one AERONET AOD retrieval is available within ± 30 min of the MODIS overpass. Each observation is represented as a vector $(\mathbf{x}^T, y_{\text{mod}}, y)$, where $\mathbf{x} \in \mathfrak{R}^{36}$ is the average reflectance values for the 36 channels over

the cloud-free pixels, y_{mod} is the average MODIS AOD at 550 nm, and y is the average AERONET AOD at 550 nm.

3. Methodology

Machine learning models have been used to retrieve AOD at given locations, because they can approximate the relationship between the spectral values and AOD. However, the physical variables (features) in machine learning models such as SVMs are often mapped to other spaces, making the learned regression model can not be explained with physical meanings. To avoid this problem, we select a linear model called ridge regression (RR) as the basic machine learning model.

As shown in [Figure 1](#), the proposed hybrid model consists of two sub-models: the DT algorithm and the RR model. The coupling process between them can be formulated as:

$$\hat{y} = \varphi(x) = y_{\text{mod}} \oplus f(\mathbf{x}; \mathbf{w}), \quad (1)$$

where y_{mod} is the DT algorithm, $f(\mathbf{x}; \mathbf{w})$ is the RR model, w is the parameter vector in the RR model, \hat{y} is the estimated AOD, and the symbol ' \oplus ' represents the coupling operation between the two sub-models. Since the sub-model y_{mod} can be obtained from the MOD04 product, we only need to introduce the basic idea of the other sub-model RR before presenting the hybrid model.

3.1. Ridge regression model

Given ℓ collocated AERONET-MODIS training samples $\{\mathbf{x}_i, y_i\}_{i=1}^{\ell}$, the main idea of linear regression is to fit a function $f(\mathbf{x}; \mathbf{w}) = \mathbf{x}^T \mathbf{w} + b$ such that the residual sum of square (loss function) is minimized: $(\mathbf{w}^*, b^*) = \arg \min_{\mathbf{w}, b} \sum_{i=1}^{\ell} \|f(\mathbf{x}_i; \mathbf{w}) - y_i\|^2$. For simplicity, we append a new element 1 to each \mathbf{x}_i . Then, the coefficient b can be absorbed into \mathbf{w} . Let $\mathbf{y} = [y_1, \dots, y_{\ell}]^T$, $\mathbf{X} = [\mathbf{x}_1, \dots, \mathbf{x}_{\ell}]^T$, where the superscript 'T' denotes the transpose of vectors or matrices, we can rewrite the loss function as a matrix form $\mathbf{w}^* = \arg \min_{\mathbf{w}} \|\mathbf{X}\mathbf{w} - \mathbf{y}\|^2$ whose solution is $\mathbf{w}^* = (\mathbf{X}^T \mathbf{X})^{-1} \mathbf{X}^T \mathbf{y}$.

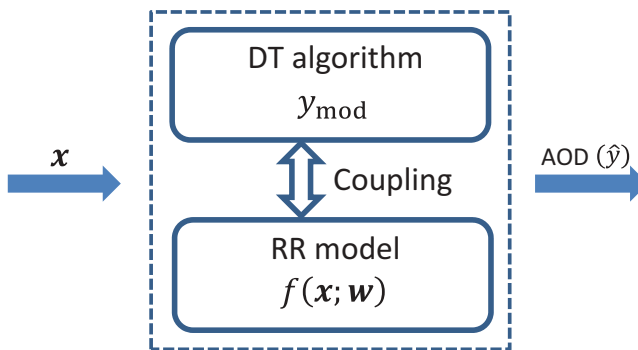


Figure 1. Schematic diagram of the hybrid model, which consists of the DT algorithm and the RR model.

For the aerosol retrieval, there are only several ground-based stations in China, resulting in limited numbers of the ground-truth AOD. Besides, the ground-based observations must match with the satellite observations in both time and space, which further reduces the available ground-truth. On the other hand, the spectral reflectances are highly correlated with each other. Thus, the covariance matrix $\mathbf{X}^T\mathbf{X}$ is often singular. One popularly adopted method to handle this issue is imposing a penalty on the norm of \mathbf{w} :

$$\mathbf{w}^* = \arg \min_{\mathbf{w}} \|\mathbf{X}\mathbf{w} - \mathbf{y}\|^2 + \alpha \|\mathbf{w}\|^2, \quad (2)$$

where α is a regularization parameter, and the solution is:

$$\mathbf{w}^* = (\mathbf{X}^T\mathbf{X} + \alpha\mathbf{I})^{-1}\mathbf{X}^T\mathbf{y}, \quad (3)$$

where \mathbf{I} is an identity matrix. The term $\alpha \|\mathbf{w}\|^2$ in Eq. (2) is called Tikhonov regularizer (Tikhonov 1963). In statistics, this regularization method is called RR.

3.2. Hybrid model

In general, there exists no generic approach to design the coupling connections. The actual coupling framework is more problem dependent and can be quite complicated, because it depends on the form in which domain knowledge is available. For aerosol retrieval, the domain knowledge can be derived from the DT algorithm. Thus, we employ two simple yet effective coupling frameworks: the serial framework shown in Figure 2(a) and the parallel framework shown in Figure 2(b).

In the serial framework, the retrieved AOD from the DT algorithm is used as a feature for the subsequent RR model, which can be written as:

$$\hat{y} = y_{mod} \oplus f(\mathbf{x}; \mathbf{w}) = f(\bar{\mathbf{x}}; \mathbf{w}), \quad (4)$$

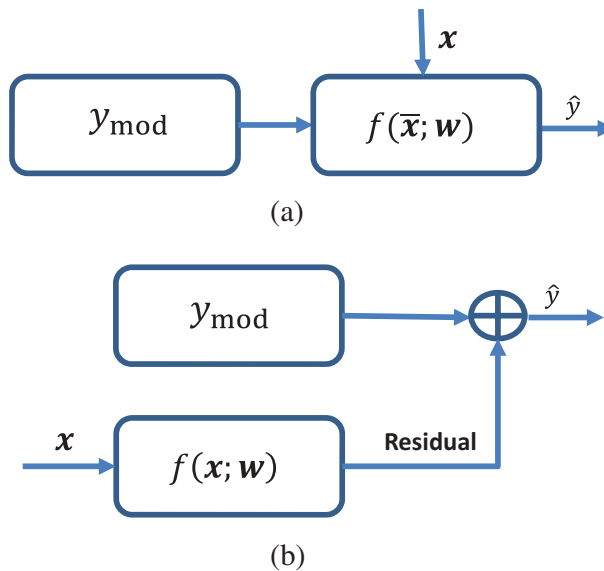


Figure 2. Two coupling frameworks: (a) the serial framework and (b) the parallel framework.

where $\bar{\mathbf{x}} = [\mathbf{x}^T, y_{\text{mod}}]^T$. The optimal parameter \mathbf{w}^* in Eq. (4) can be derived according to Eq. (3). In the testing stage, we firstly compute the initial AOD by the DT algorithm, and then estimate the final AOD value as $\hat{y}_t = \bar{\mathbf{x}}_t^T \mathbf{w}^*$. Similar to (Lary et al. 2009), the RR model plays an important role to correct the retrieval bias. More importantly, all spectral reflectance values are fed into the RR model, including the values that are not used in the physical model, making the framework obtains higher performance and can indicate the importance of each channel.

In the parallel framework, the RR model is applied to learn the residual between the retrieved AOD by the DT algorithm and the ground-truth AOD, which can be written as:

$$\hat{y} = y_{\text{mod}} \oplus f(\mathbf{x}; \mathbf{w}) = y_{\text{mod}} + f(\mathbf{x}; \mathbf{w}). \quad (5)$$

Thus, the ground-truth for the RR model is $y - y_{\text{mod}}$, instead of y . The optimal parameter \mathbf{w}^* in Eq. (5) can also be derived according to Eq. (3). In the testing stage, we firstly compute the residual by the RR model, and then estimate the final AOD value as $\hat{y}_t = y_{\text{mod}} + \mathbf{x}_t^T \mathbf{w}^*$.

To demonstrate the superiority of the two coupling frameworks, we compare them with the two sub-models: DT and RR. The regularization parameter α in the RR model is chosen from $\{10^{-3}, \dots, 10^3\}$ via a five-fold cross validation. In all the experiments, we randomly divide the data from each station into the training set and the testing set. The training set is used to train the parameters in the RR model, whereas the testing set is used to evaluate the performance of each model. In order to reduce the effect of random selection, all the algorithms are repeated 10 times and average performances are reported. Without loss of generality, we use two mainstream evaluation metrics: the root mean square error (RMSE) to evaluate the accuracy of the estimations, and the Pearson's correlation coefficient r to evaluate the goodness of fit.

4. Experimental results

In order to analyze the effect of α on the retrieval performance achieved by three RR related models, we take Beijing and XiangHe stations as an example to establish the experiment. Figure 3 shows the experimental results using 50% samples as the training set and the rest as the testing set. As α increases, RMSE firstly decreases and then increases. Thus, the optimal α value is set to 10^{-1} in the following experiments.

Figure 4 demonstrates the performance of different models in terms of average r values and standard deviations using different numbers of training samples from 10 stations. From this figure, several conclusions can be observed. First, as the number of training samples increases, the r values achieved by RR, serial and parallel frameworks increase, while those achieved by DT are relatively stable. This indicates that the performance of physical models don't depend on the available data. Second, when the percent of training samples is 10%, RR obtains inferior performance as compared to DT, because it is difficult to train a strong machine learning model with such a small number of training samples. Similarly, the residual between the retrieved AOD from DT and the ground-truth AOD can not be accurately learned by RR, thus the parallel framework is a little worse than DT. Different from RR and the parallel framework, the serial framework considers the retrieved AOD by DT as a feature. This powerful feature

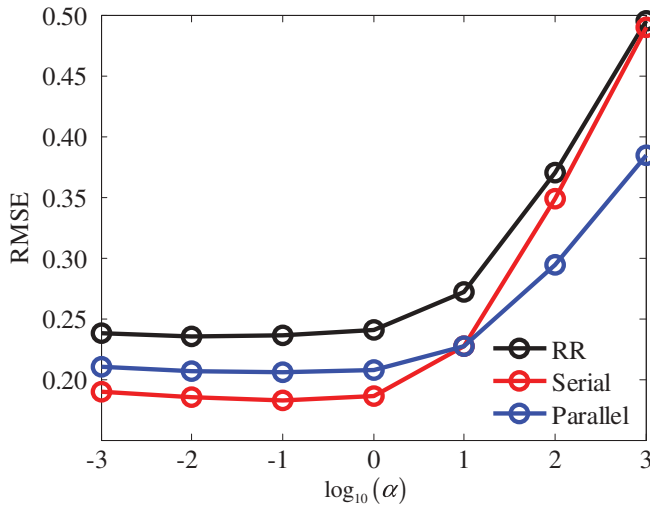


Figure 3. Effects of parameter α on the retrieval performance.

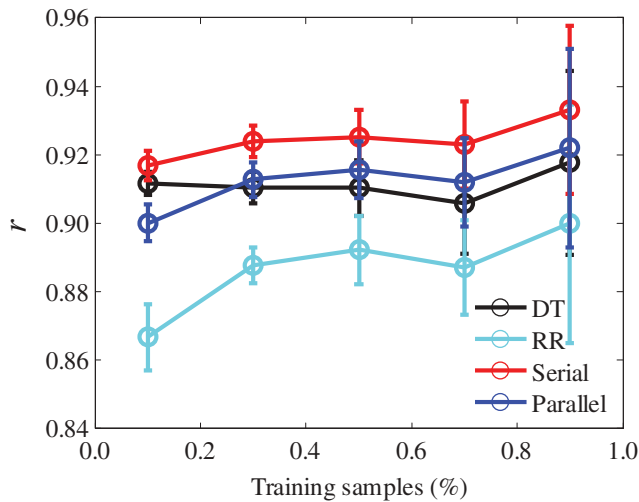


Figure 4. r and standard deviations achieved by applying four different methods under different numbers of training samples. Standard deviations are shown as the error bars in the vertical direction.

will be given a large weight to effectively address the issue of small training samples, making the serial framework a little better than DT. The last but not the least, when the percent of training samples exceeds 10%, DT achieves higher performance than RR in most cases, because RR is a linear model, failing to adequately model the complex non-linear relationship between the spectral reflectance and AOD. In contrast, the serial and parallel frameworks are capable of correcting the bias between the ground-truth AOD and the retrieved one, thus achieving better performance than DT. This sufficiently certifies the effectiveness of the proposed frameworks. Besides, the serial framework

may be a more promising one, because it attains superior performance than the parallel framework.

All the aforementioned conclusions can be further recognised from another evaluation metric RMSE in Figure 5, where the smaller values correspond to the better performance. In addition, Figure 6 shows the scatter plot of the retrieved AOD by the

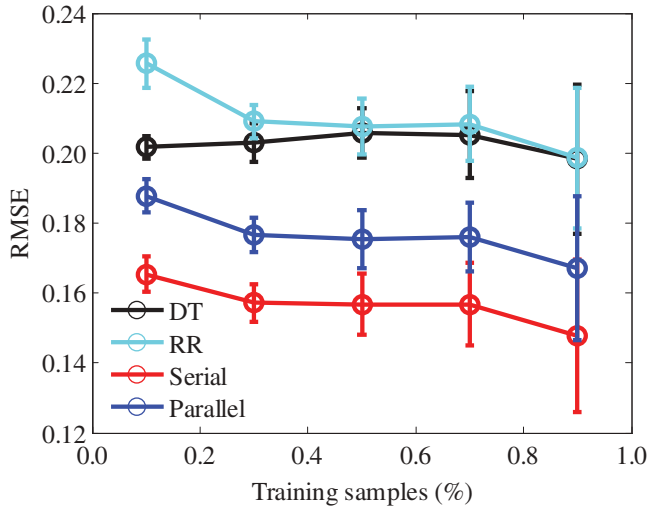


Figure 5. RMSE and standard deviations achieved by applying four different methods under different numbers of training samples. Standard deviations are shown as the error bars in the vertical direction.

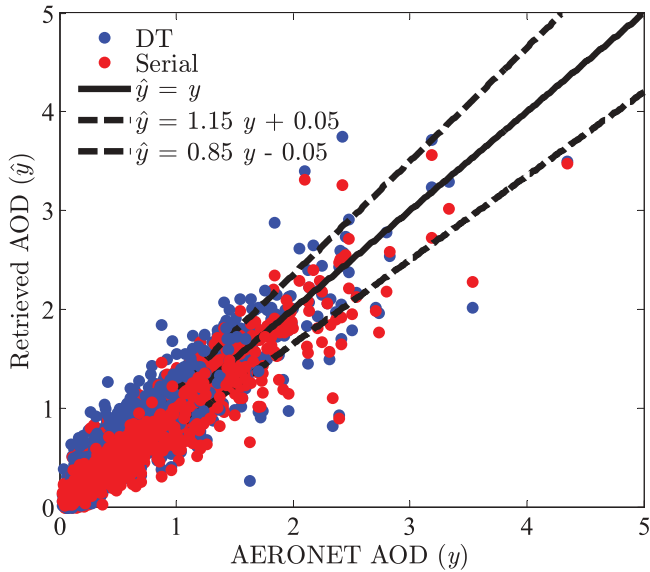


Figure 6. Scatter plot of the retrieved AOD at $\lambda = 550$ nm by the serial framework and DT versus the ground-truth using 50% training samples. Ideal retrievals are represented by a solid line, while dashed lines correspond to boundaries of a region of acceptable retrievals.

serial framework and DT versus the ground-truth AOD. It is demonstrated that the retrieved AOD values by the serial framework are closer to the ideal ones than those by DT, especially when the ideal AOD values are small. Besides, for the serial framework, there are more numbers of points that fall into the region of acceptable retrievals (Ristovski, Vucetic, and Obradovic 2012; Remer et al. 2005) than DT. Similar conclusions can be observed from Figure 7, which demonstrates the scatter plot of the retrieved AOD by the parallel framework and DT versus the ground-truth AOD.

We also test the robustness of the proposed frameworks on surface types and seasons of observations. Similar to Figure 3, we use Beijing and XiangHe stations to construct experiments, because they have more numbers of samples than other stations (i.e., 843 observations at Beijing site and 674 observations at XiangHe site). Table 1 lists the number of observations in different seasons. We test on one season data and train different models on the remaining three seasons. The detailed performance of different models in terms of RMSE and r are reported in Tables 2 and 3 respectively, where the best results are highlighted by bold fonts. From these tables, we can observe that the serial framework achieves superior performance than the other models in three seasons,

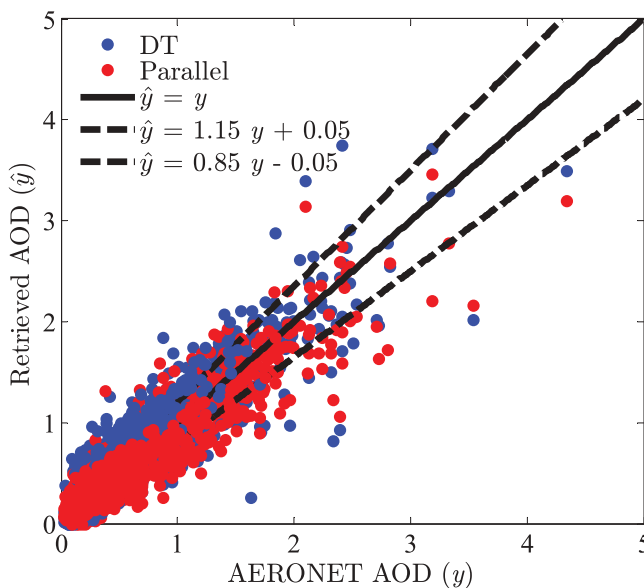


Figure 7. Scatter plot of the retrieved AOD at $\lambda = 550$ nm by the parallel framework and DT versus the ground-truth using 50% training samples. Ideal retrievals are represented by a solid line, while dashed lines correspond to boundaries of a region of acceptable retrievals.

Table 1. Sample distributions in different seasons at Beijing and XiangHe stations.

Season	Months	No. of observations
Spring	Mar-May	443
Summer	Jun-Aug	441
Autumn	Sep-Nov	578
Winter	Dec-Feb	55
Total	–	1517

Table 2. RMSE comparison by season using four different methods at Beijing and XiangHe stations.

Method	Spring	Summer	Autumn	Winter	Average
DT	0.2044	0.2777	0.1670	0.0637	0.1728
RR	0.2099	0.3027	0.1988	0.1498	0.2153
Parallel	0.1724	0.2517	0.1368	0.0617	0.1557
Serial	0.1557	0.2429	0.1364	0.0990	0.1585

Table 3. r comparison by season using four different methods at Beijing and XiangHe stations.

Method	Spring	Summer	Autumn	Winter	Average
DT	0.9285	0.9230	0.9478	0.9298	0.9323
RR	0.8747	0.8998	0.9164	0.5609	0.8130
Parallel	0.9337	0.9322	0.9612	0.9461	0.9433
Serial	0.9381	0.9366	0.9621	0.8459	0.9207

Table 4. PAR comparison by season using four different methods at Beijing and XiangHe stations.

Method	Spring	Summer	Autumn	Winter	Average
DT	0.4944	0.4989	0.6765	0.8182	0.6220
RR	0.4673	0.4739	0.4983	0.3636	0.4508
Parallel	0.6682	0.5964	0.7751	0.8727	0.7281
Serial	0.6275	0.6009	0.6972	0.6364	0.6405

Table 5. RMSE comparison by station using four different methods at Beijing and XiangHe stations.

Station	DT	RR	Parallel	Serial
Beijing	0.2406	0.2861	0.2199	0.2160
XiangHe	0.1726	0.2764	0.1601	0.2086
Average	0.2066	0.2812	0.1900	0.2123

Table 6. r comparison by station using four different methods at Beijing and XiangHe stations.

Station	DT	RR	Parallel	Serial
Beijing	0.9103	0.8593	0.9147	0.9217
XiangHe	0.9592	0.8701	0.9603	0.9411
Average	0.9348	0.8647	0.9375	0.9314

Table 7. PAR comparison by station using four different methods at Beijing and XiangHe stations.

Station	DT	RR	Parallel	Serial
Beijing	0.4958	0.4069	0.5836	0.5065
XiangHe	0.6780	0.3724	0.7404	0.5718
Average	0.5869	0.3897	0.6620	0.5392

while the parallel framework is a little better than the serial one in terms of average performance due to the accurate prediction in the winter season. Besides, Table 4 shows the proportion of data number within the acceptable region (PAR). It can be observed that the parallel and serial frameworks can obtain more numbers of acceptable retrievals than DT and RR. Similarly, Tables 5–7 demonstrate the performances of different models on different stations, where one station is used as the training set and the other one as the testing set. Once again, the parallel framework obtains the highest performance than the other models.

5. Conclusion

This paper proposes two frameworks to correct the MODIS AOD product using the RR model. In the serial framework, we use the retrieved AOD from the DT algorithm as a powerful feature for the RR model. In the parallel framework, the RR model is used to learn the residual between the retrieved AOD from the DT algorithm and the ground-truth AOD. The experimental results on ten aerosol sites demonstrate that the proposed two frameworks can effectively correct the retrieval bias caused by the DT algorithm. Besides, the serial framework exhibits superior performance than the parallel one in most cases, while the parallel framework is more robust to surface types and seasons of observations.

Acknowledgments

The authors would like to thank the Atmospheric Sciences Data Centre at NASA Goddard Space Flight Centre for help with the MODIS data, and the AERONET Principal Investigators for providing the ground-based aerosol data.

Disclosure statement

No potential conflict of interest was reported by the authors.

Funding

This work was supported in part by the Natural Science Foundation of China under Grant Numbers: 61532009 and 41501377, and in part by the Natural Science Foundation of Jiangsu Province, China, under Grant 15KJA520001.

References

- Chu, D. A., Y. J. Kaufman, C. Ichoku, L. A. Remer, D. Tanr, and B. N. Holben. 2002. "Validation of MODIS Aerosol Optical Depth Retrieval over Land." *Geophysical Research Letters* 29 (12): 8007. doi:10.1029/2001GL013205.
- Dubovik, O., A. Smirnov, B. N. Holben, M. D. King, Y. J. Kaufman, T. F. Eck, and I. Slutsker. 2000. "Accuracy Assessments of Aerosol Optical Properties Retrieved from Aerosol Robotic Network (AERONET) Sun and Sky Radiance Measurements." *Journal of Geophysical Research Atmospheres* 105 (D8): 9791–9806. doi:10.1029/2000JD900040.
- Fan, X. R., M. Z. Kang, E. Heuvelink, P. De Reffye, and B. G. Hu. 2015. "A Knowledge-And-Data-Driven Modeling Approach for Simulating Plant Growth: A Case Study on Tomato Growth." *Ecological Modelling* 312: 363–373. doi:10.1016/j.ecolmodel.2015.06.006.
- Gao, L., J. Li, L. Chen, L. Zhang, and A. K. Heidinger. 2016. "Retrieval and Validation of Atmospheric Aerosol Optical Depth from AVHRR over China." *IEEE Transactions on Geoscience and Remote Sensing* 54 (11): 6280–6291. doi:10.1109/TGRS.2016.2574756.
- Hang, R., Q. Liu, H. Song, and Y. Sun. 2017. "Graph Regularized Nonlinear Ridge Regression for Remote Sensing Data Analysis." *IEEE Journal of Selected Topics in Applied Earth Observations and Remote Sensing* 10(1): 277–285.
- Holben, B. N., T. F. Eck, I. Slutsker, D. Tanr, J. P. Buis, A. Setzer, E. Vermote, J. A. Reagan, Y. J. Kaufman, and T. Nakajima. 1998. "AERONETA Federated Instrument Network and Data Archive for Aerosol Characterization." *Remote Sensing of Environment* 66 (1): 1–16. doi:10.1016/S0034-4257(98)00031-5.

- Huang, G., C. Huang, Z. Li, and H. Chen. 2015. "Development and Validation of a Robust Algorithm for Retrieving Aerosol Optical Depth over Land from MODIS Data." *IEEE Journal of Selected Topics in Applied Earth Observations and Remote Sensing* 8 (3): 1152–1166.
- Kaufman, Y. J., D. Tanr, and O. Boucher. 2002. "A Satellite View of Aerosols in the Climate System." *Nature* 419 (6903): 215–223. doi:10.1038/nature01091.
- King, M. D., Y. J. Kaufman, W. Paul Menzel, and D. Tanr. 1992. "Remote Sensing of Cloud, Aerosol, and Water Vapor Properties from the Moderate Resolution Imaging Spectrometer (MODIS)." *IEEE Transactions on Geoscience and Remote Sensing* 30 (1): 2–27. doi:10.1109/36.124212.
- Lary, D. J., L. A. Remer, D. Macneill, and B. Roscoe. 2009. "Machine Learning and Bias Correction of MODIS Aerosol Optical Depth." *IEEE Geoscience and Remote Sensing Letters* 6 (4): 694–698. doi:10.1109/LGRS.2009.2023605.
- Levy, R. C., S. Mattoo, L. A. Munchak, and L. A. Remer. 2013. "The Collection 6 MODIS Aerosol Products over Land and Ocean." *Atmospheric Measurement Techniques* 6 (1): 2989–3034. doi:10.5194/amt-6-2989-2013.
- Nguyen, T., N. Thanh, S. Mantovani, and P. Campalani. 2011. "Validation of Support Vector Regression in Deriving Aerosol Optical Thickness Maps at 1 Km² Spatial Resolution from Satellite Observations." *IEEE International Symposium on Signal Processing and Information Technology*, 143–153.
- Petrenko, M., C. Ichoku, and G. Leptoukh. 2012. "Multi-Sensor Aerosol Products Sampling System (MAPSS)." *Atmospheric Measurement Techniques* 5 (5): 913–926. doi:10.5194/amt-5-913-2012.
- Qu, H. B., and B. G. Hu. 2009. "Variational Learning for Generalized Associative Functional Networks in Modeling Dynamic Process of Plant Growth \hat{p} \hat{p} ." *Ecological Informatics* 4 (3): 163–176. doi:10.1016/j.ecoinf.2009.06.004.
- Remer, L. A., Y. J. Kaufman, D. Tanr, S. Mattoo, D. A. Chu, J. V. Martins, R. R. Li, C. Ichoku, R. C. Levy, and R. G. Kleidman. 2005. "The MODIS Aerosol Algorithm, Products, and Validation." *Journal of the Atmospheric Sciences* 62 (4): 947–973. doi:10.1175/JAS3385.1.
- Ristovski, K., S. Vucetic, and Z. Obradovic. 2012. "Uncertainty Analysis of Neural-Network-Based Aerosol Retrieval." *IEEE Transactions on Geoscience and Remote Sensing* 50 (2): 409–414. doi:10.1109/TGRS.2011.2166120.
- Sun, Y., R. Hang, Q. Liu, F. Zhu, and H. Pei. 2016. "Graph-Regularized Low-Rank Representation for Aerosol Optical Depth Retrieval." *International Journal of Remote Sensing* 37 (24): 5749–5762. doi:10.1080/01431161.2016.1249302.
- Tikhonov, A. N. 1963. "Regularization of Incorrectly Posed Problems." *Sov Mathematical* 4 (1): 1624–1627.
- Vucetic, S., B. Han, M. Wen, and L. Zhanqing. 2008. "A Data-Mining Approach for the Validation of Aerosol Retrievals." *IEEE Geoscience and Remote Sensing Letters* 5 (1): 113–117. doi:10.1109/LGRS.2007.912725.